Electronic Supplementary Material (ESI) for RSC Advances.

Host–guest complexation between 1,4-dipropoxypillar[5]arene and imidazolium-based ionic liquids †

Lingyan Gao,[a] Yong Yao,[a] Shengyi Dong,*[a] and Jiayin Yuan*[b]

[a]*Department of Chemistry, Zhejiang University, Hangzhou 310027, P. R. China*
Fax: +86-571-8795-1895; Tel: +86-571-8795-3189; Email address: dongsyzju@zju.edu.cn.
[b]*Max Planck Institute of Colloids and Interfaces, Potsdam 14476, Germany,*
Jiayin.Yuan@mpikg.mpg.de

Electronic Supplementary Information (16 pages)

1. Materials and methods

All reagents were commercially available and used as supplied without further purification. 1,4-Dipropoxybenzene[S1a] **DPP5**[S1b] and 1,4-bis(2-bromoethoxy)benzene[S1c] were synthesized according to literature procedures. ^{1}H NMR spectra were collected on a temperature-controlled Bruker AVANCE DMX-400 spectrometer. ^{13}C NMR spectra were recorded on a Bruker AVANCE DMX-400 spectrometer at 100 MHz. Low-resolution electrospray ionization (LRESI) mass spectra were obtained on a Bruker Esquire 3000 plus mass spectrometer (Bruker-Franzen Analytik GmbH Bremen, Germany) equipped with an ESI interface and an ion trap analyzer.

*2. Synthesis s of AB_2 monomer **3***

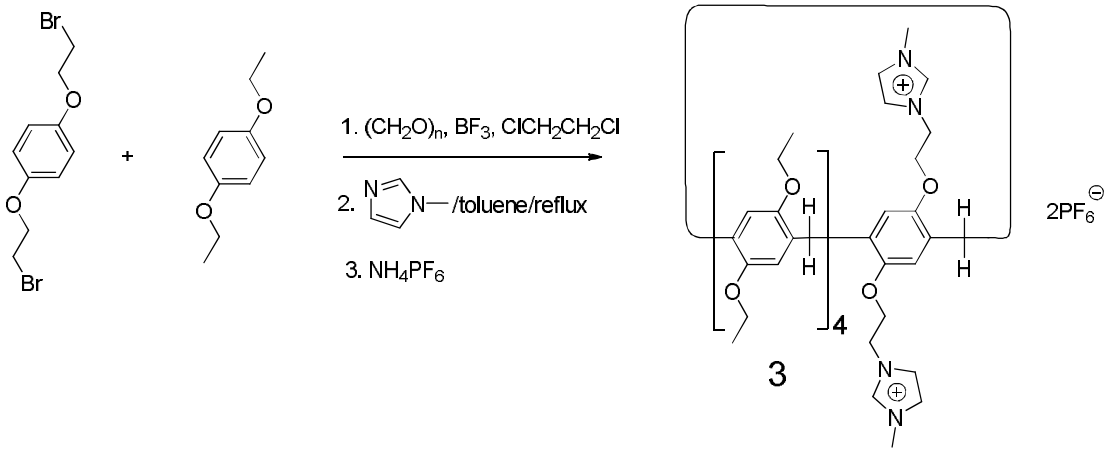

A mixture of 1,4-bis(2-bromoethoxy)benzene (1.60 g, 5.00 mmol), 1,4-diethoxybenzene (8.30 g, 50.0 mmol), boron trifluoride etherate (12 mL), paraformaldehyde (5.70 g, 150 mmol) and $ClCH_2CH_2Cl$ (500 mL) was stirred at room temperature for half an hour. Then a saturated aqueous solution of $NaHCO_3$ was dropped to the mixture. After filteration, the organic layer was separated, washed with water and brine, and dried over Na_2SO_4. The solvent was removed to get a white solid, which was used for the next step without further purification. This white solid and 1-methyl-1H-imidazole (8.20 g, 100 mmol) was stirred under reflux in toluene overnight. The solution was evaporated under vacuo and the residue was dissolved in water. A saturated aqueous solution of NH_4PF_6 was added to afford a white solid, which was purified by chromatography on silica gel ($CH_3COOC_2H_5/CH_3CN$, *v*/*v* 4:1 → 2:1) to obtain **3**. (1.10 g, 25%). Melting point: 137.5–140.1 °C. ^{1}H NMR (400 MHz, CD_3CN, 295 K) δ (ppm): 7.25 (2H, s), 6.98 (4H, J = 4.0 Hz, d), 6.87 (2H, s),

6.76 (4H, J = 4.0 Hz, d), 6.58 (2H, s), 6.24 (2H, s), 4.38 (4H, J = 4.0 Hz, t), 4.29 (4H, J = 4.0 Hz, t), 3.97–3.88 (12H, m), 3.82–3.76 (8H, m), 3.67 (2H, s), 3.65 (4H, s), 2.86 (6H, s), 1.42–1.37 (24H, m). ^{13}C NMR (100 MHz, CD_3CN, 295 K) δ (ppm): 149.70, 149.41, 149.24, 149.03, 148.41, 135.34, 129.17, 128.26, 128.10, 127.94, 127.79, 123.16, 121.68, 114.73, 114.45, 114.23, 113.57, 113.37, 65.09, 64.07, 63.79, 63.61, 63.35, 49.48, 34.49, 29.11, 28.81, 28.59, 14.35, 14.27. LRESIMS: m/z 1197.6 $[M - PF_6]^+$ (36%), m/z 1051.8 $[M - 2HPF_6 - H]^+$ (100%). HRESIMS: m/z calcd for $[M - PF_6]^+$ $C_{63}H_{80}F_6N_4O_{10}P^+$, 1197.5516; found 1197.5504; error –1.2 ppm.

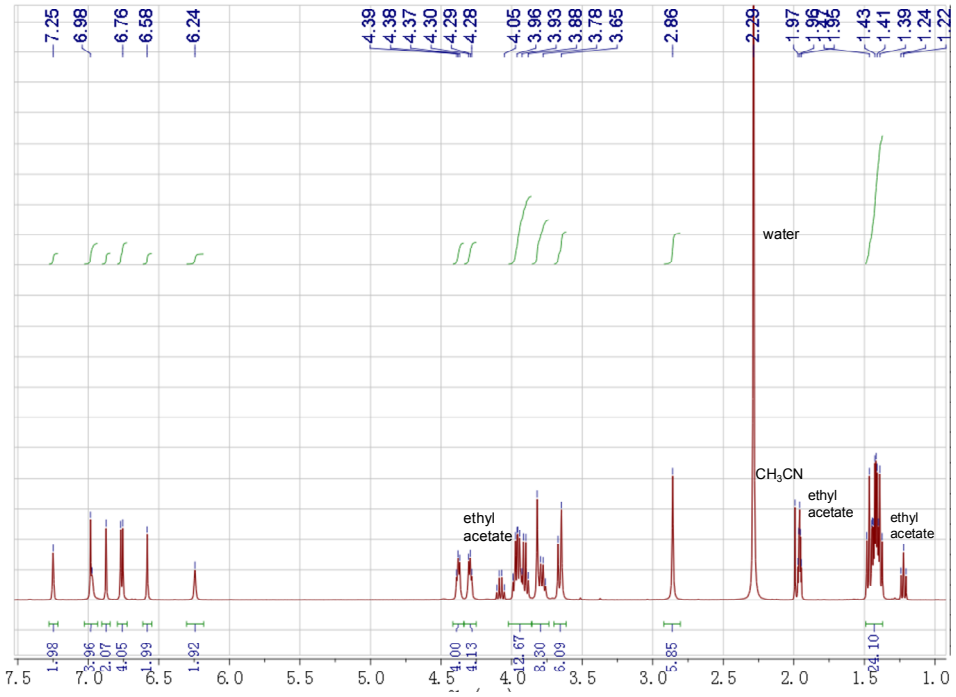

Fig. S1 ^{1}H NMR spectrum (400 MHz, CD_3CN, 22 °C) of **3**.

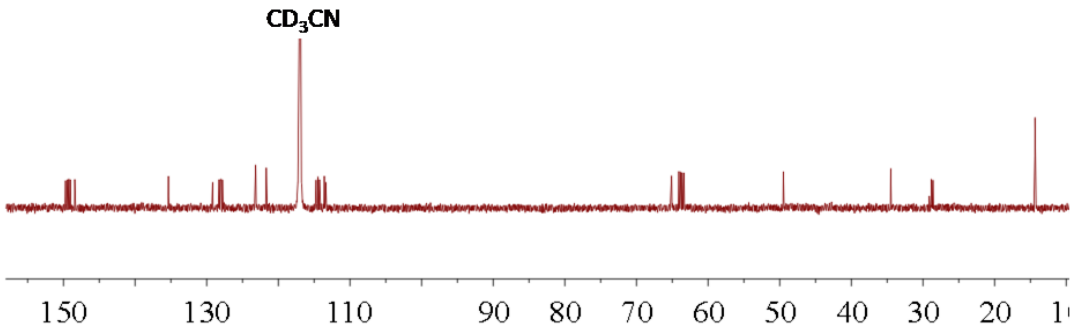

Fig. S2 ^{13}C NMR spectrum (100 MHz, CD_3CN, 22 °C) of **3**.

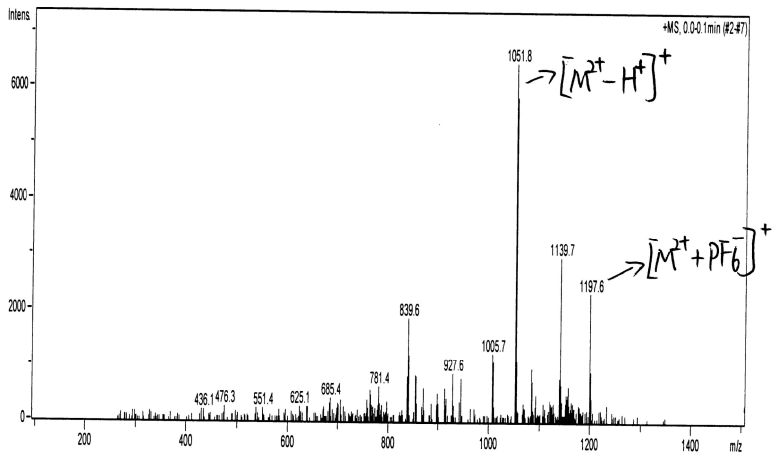

Fig. S3 LRESI mass spectrum of **3**.

*3. 2D NOESY spectrum of an equimolar mixture of **DPP5** and **2a***

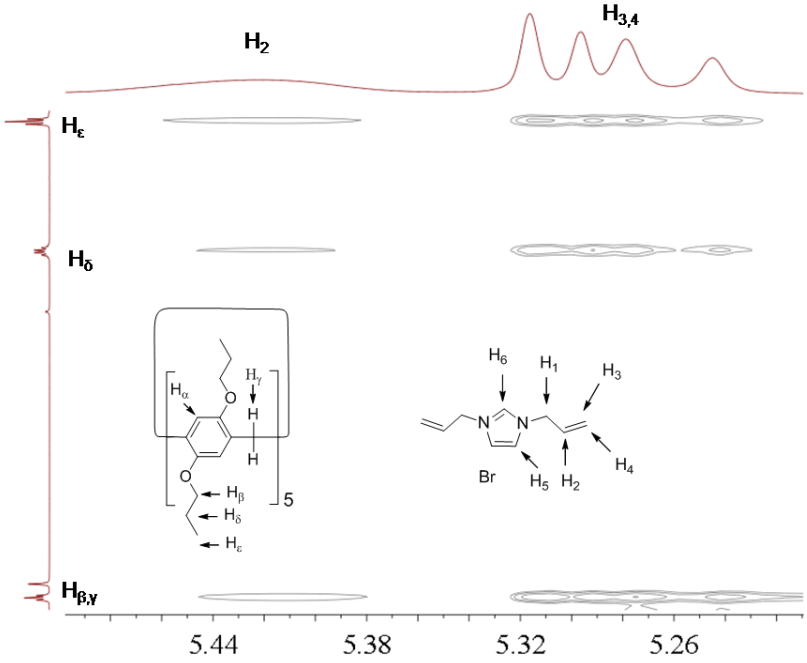

Fig. S4 Partial 2D NOESY spectrum of an equimolar mixture of **DPP5** and **2a** (400 MHz, $CDCl_3$, 22 °C).

*4. Stoichiometry and association constants determination for the complexation between **DPP5** and **2a–g***

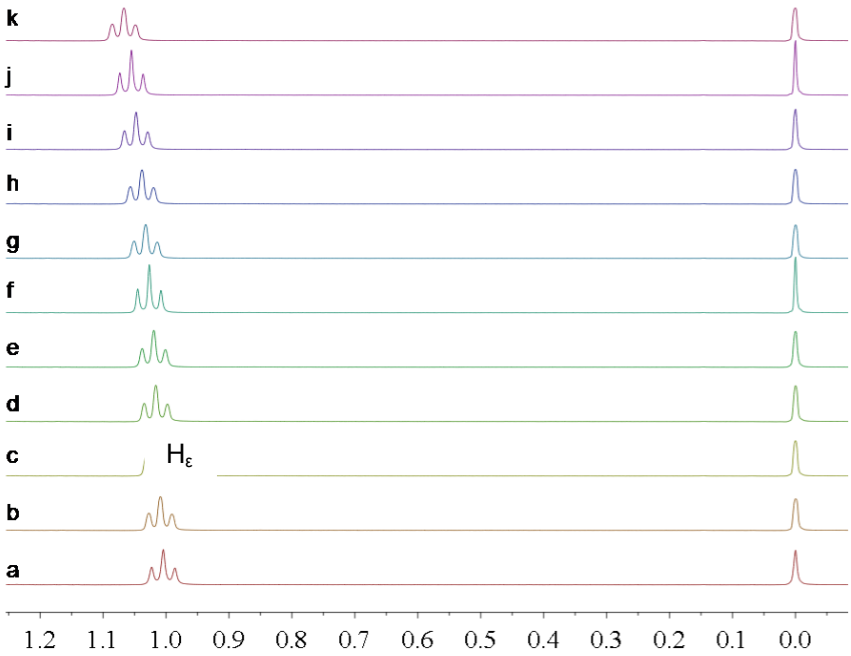

Fig. S5 Partial ^{1}H NMR spectra (400 MHz, $CDCl_3$, 22 °C) of **DPP5** at a constant concentration of 2.00 mM upon addition of **G** (**2a**, 15 mM): (a) 0.00 μL, (b) 10.0 μL to a, (c) 10.0 μL to b, (d) 10.0 μL to c, (e) 10.0 μL to d, (f) 25.0 μL to e, (g) 25.0 μL to f, (h) 25.0 μL to g, (i) 50.0 μL to h, (j) 50.0 μL to i, (k) 100 μL to j, (l) 100 μL to k.

To determine the stoichiometry and association constant between **DPP5** and **2a** (**G**), NMR titrations were done with solutions which had a constant concentration of **DPP5** (2 mM) and varying concentrations of **G**. By a non-linear curve-fitting method, the association constant (K_a) of **DPP5**⊃**2a** was estimated to be about 9.50 (± 0.16) × 10 M^{-1}. By a mole ratio plot, a 1:1 stoichiometry was obtained.

The non-linear curve-fitting was based on the equation:[S2]

$$\Delta\delta = (\Delta\delta_\infty/[H]_0)\,(0.5[G]_0 + 0.5([H]_0+1/K_a)-(0.5\,([G]_0^2+(2[G]_0(1/K_a - [H]_0)) + (1/K_a + [H]_0)^2)^{0.5}))$$

(Eq. S1)

Where $\Delta\delta$ is the chemical shift change of H_ε on **DPP5** at $[G]_0$, $\Delta\delta_\infty$ is the chemical shift change of H_ε when the host is completely complexed, $[H]_0$ is the fixed initial concentration of the host, and $[G]_0$ is the initial concentration of **G**.

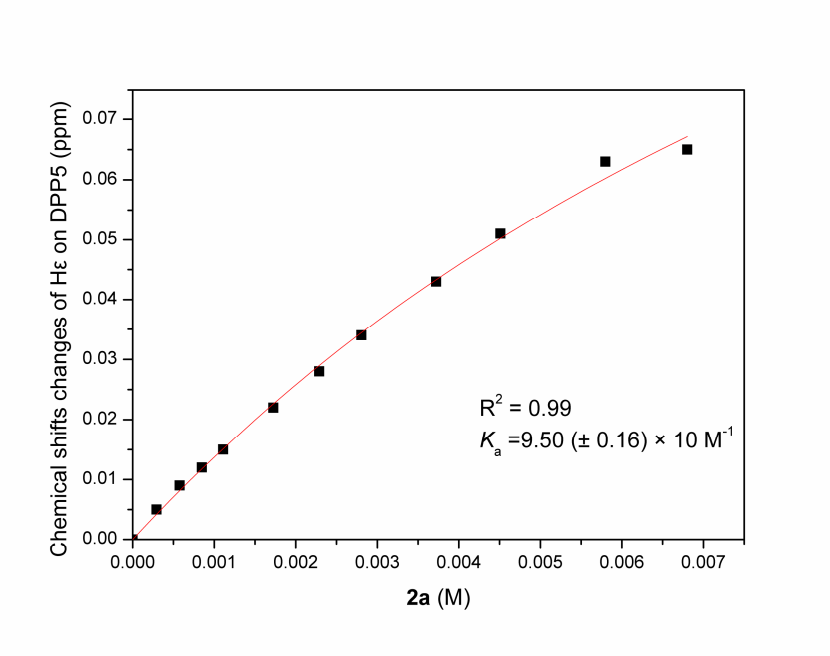

Fig. S6 The chemical shift changes of H_ε on **DPP5** upon addition of **2a**.

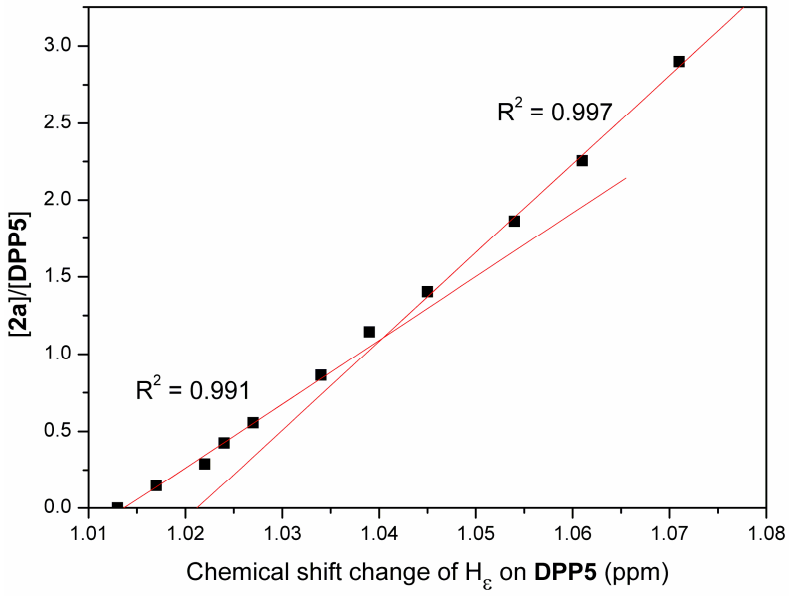

Fig. S7 Mole ratio plot for the complexation between **DPP5** and **2a**, indicating a 1:1 stoichiometry.

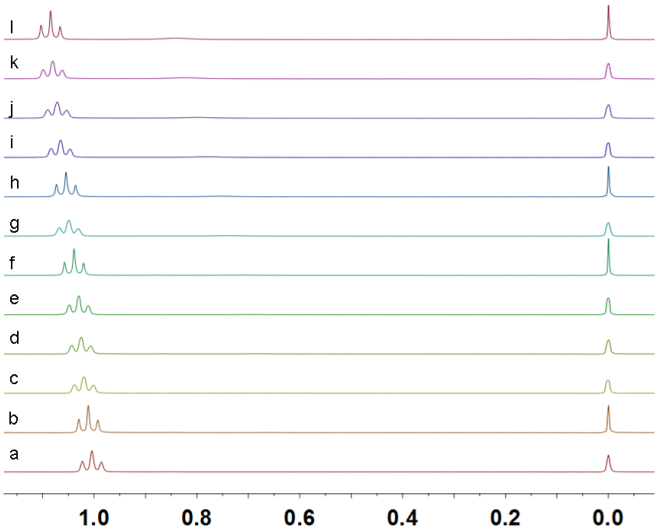

Fig. S8 Partial ^{1}H NMR spectra (400 MHz, $CDCl_3$, 22 °C) of **DPP5** at a constant concentration of 2.00 mM upon addition of **G** (**2b**, 15 mM): (a) 0.00 μL, (b) 10.0 μL to a, (c) 10.0 μL to b, (d) 10.0 μL to c, (e) 10.0 μL to d, (f) 25.0 μL to e, (g) 25.0 μL to f, (h) 25.0 μL to g, (i) 50.0 μL to h, (j) 50.0 μL to i, (k) 100 μL to j, (l) 100 μL to k.

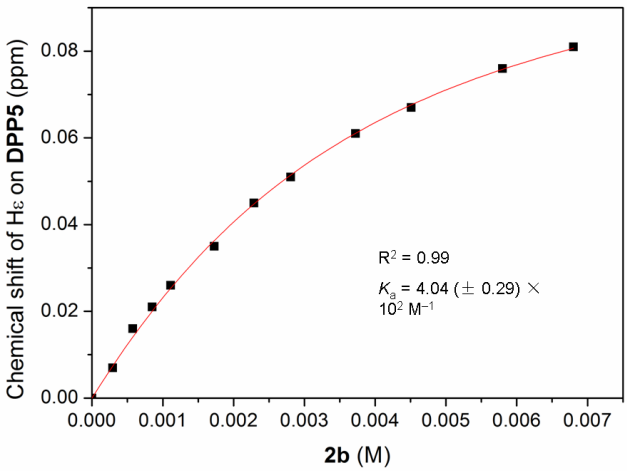

Fig. S9 The chemical shift changes of H_ε on **DPP5** upon addition of **2b**.

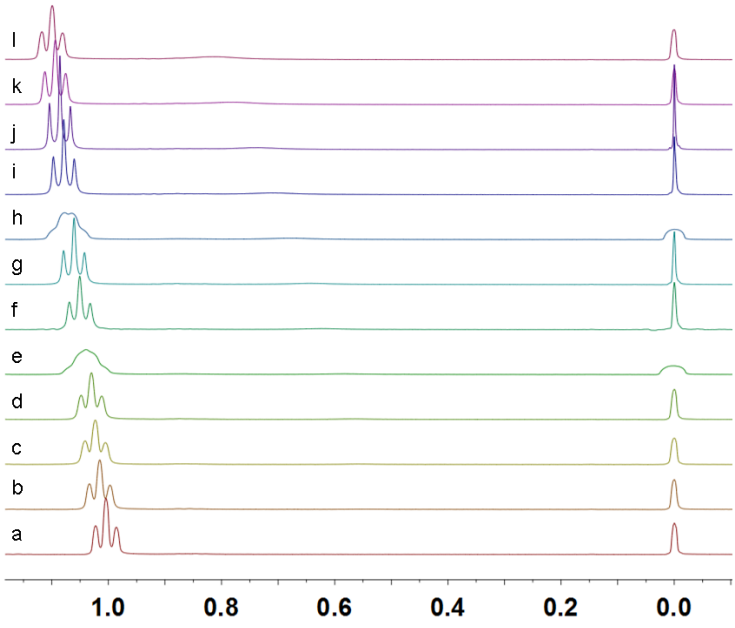

Fig. S10 Partial ^{1}H NMR spectra (400 MHz, $CDCl_3$, 22 °C) of **DPP5** at a constant concentration of 2.00 mM upon addition of **G** (**2c**, 15 mM): (a) 0.00 μL, (b) 10.0 μL to a, (c) 10.0 μL to b, (d) 10.0 μL to c, (e) 10.0 μL to d, (f) 25.0 μL to e, (g) 25.0 μL to f, (h) 25.0 μL to g, (i) 50.0 μL to h, (j) 50.0 μL to i, (k) 100 μL to j, (l) 100 μL to k.

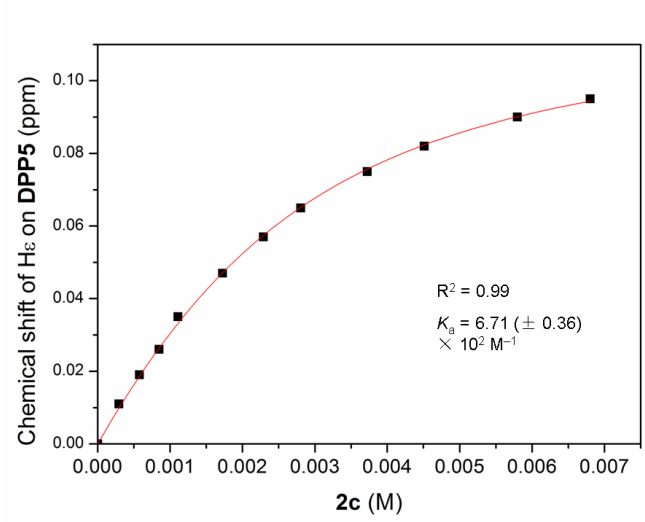

Fig. S11 The chemical shift changes of H_ε on **DPP5** upon addition of **2c**.

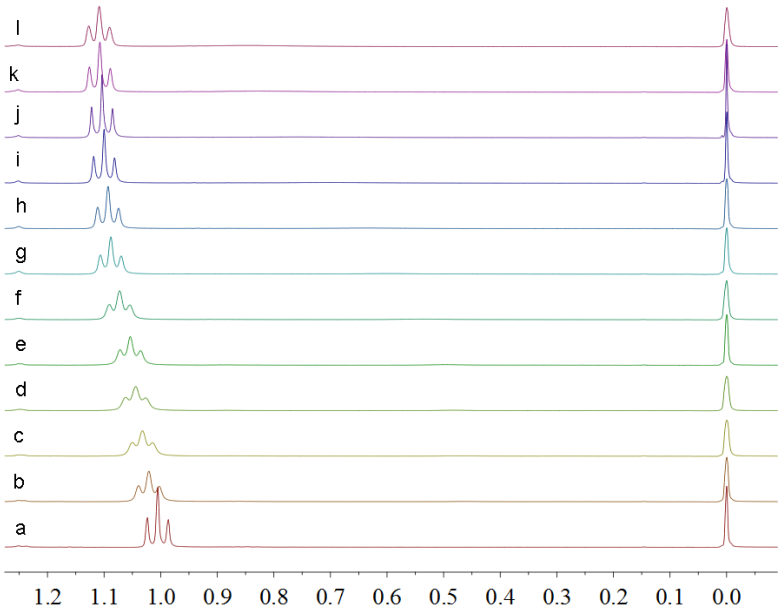

Fig. S12 Partial ^{1}H NMR spectra (400 MHz, $CDCl_3$, 22 °C) of **DPP5** at a constant concentration of 2.00 mM upon addition of **G** (**2d**, 15 mM): (a) 0.00 μL, (b) 10.0 μL to a, (c) 10.0 μL to b, (d) 10.0 μL to c, (e) 10.0 μL to d, (f) 25.0 μL to e, (g) 25.0 μL to f, (h) 25.0 μL to g, (i) 50.0 μL to h, (j) 50.0 μL to i, (k) 100 μL to j, (l) 100 μL to k.

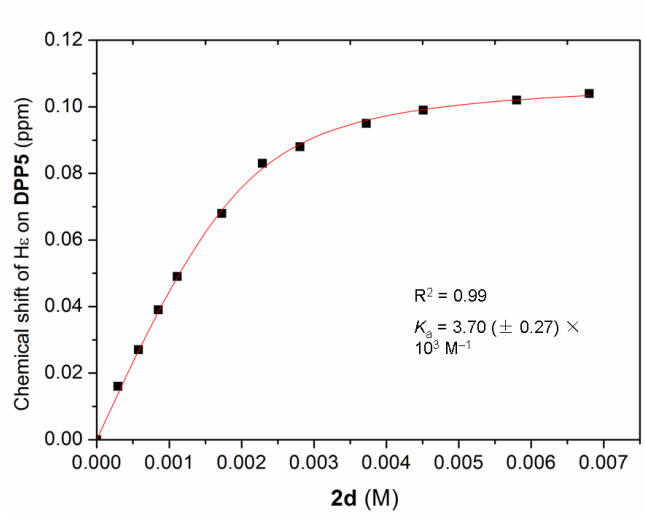

Fig. S13 The chemical shift changes of H_ε on **DPP5** upon addition of **2d**.

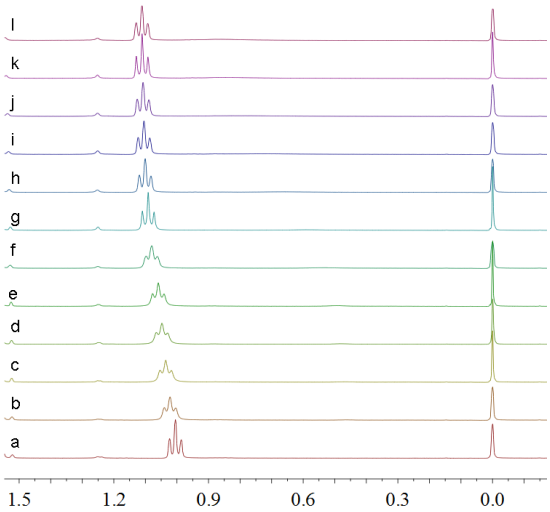

Fig. S14 Partial ^{1}H NMR spectra (400 MHz, $CDCl_3$, 22 °C) of **DPP5** at a constant concentration of 2.00 mM upon addition of **G** (**2e**, 15 mM): (a) 0.00 μL, (b) 10.0 μL to a, (c) 10.0 μL to b, (d) 10.0 μL to c, (e) 10.0 μL to d, (f) 25.0 μL to e, (g) 25.0 μL to f, (h) 25.0 μL to g, (i) 50.0 μL to h, (j) 50.0 μL to i, (k) 100 μL to j, (l) 100 μL to k.

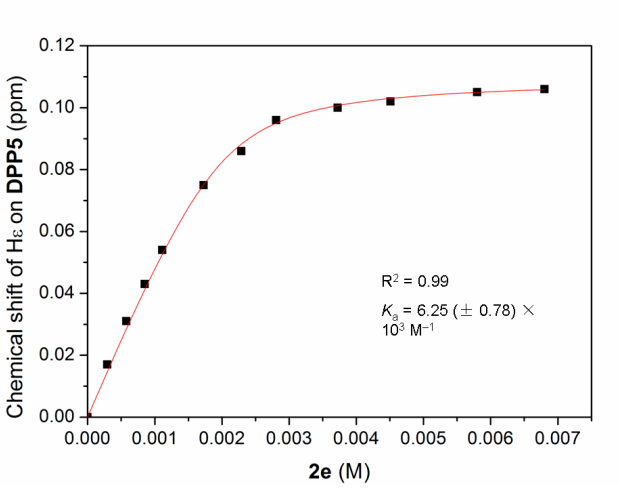

Fig. S15 The chemical shift changes of H_ε on **DPP5** upon addition of **2e**.

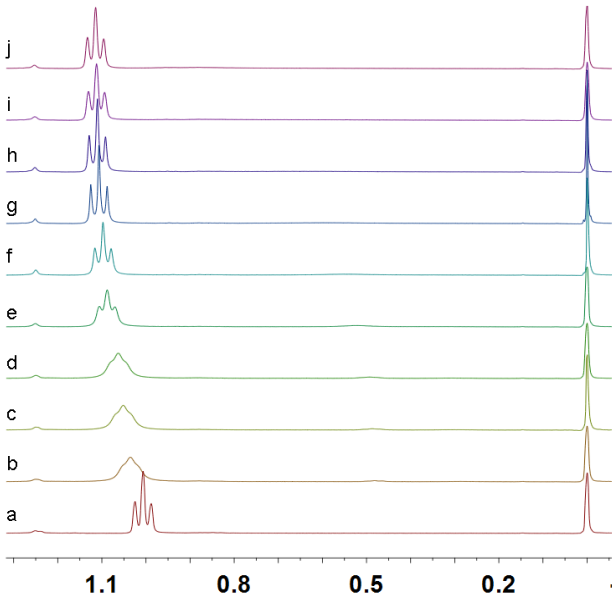

Fig. S16 Partial ^{1}H NMR spectra (400 MHz, $CDCl_3$, 22 °C) of **DPP5** at a constant concentration of 2.00 mM upon addition of **G** (**2f**, 15 mM): (a) 0.00 μL, (b) 20.0 μL to a, (c) 10.0 μL to b, (d) 10.0 μL to c, (e) 25.0 μL to d, (f) 50.0 μL to e, (g) 50.0 μL to f, (h) 50.0 μL to g, (i) 100.0 μL to h, (j) 100.0 μL to i.

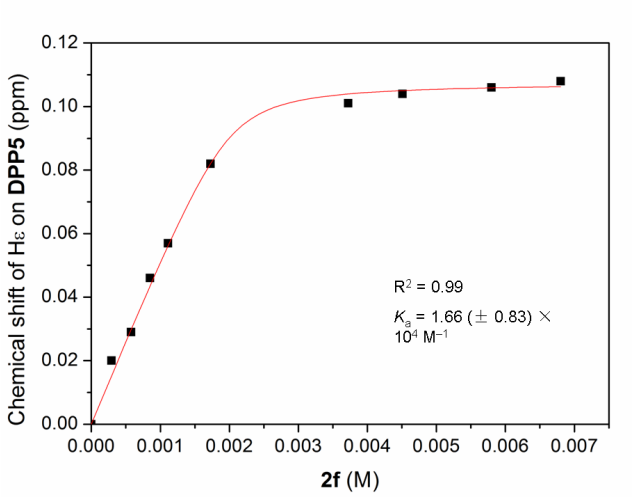

Fig. S17 The chemical shift changes of H_ε on **DPP5** upon addition of **2f**.

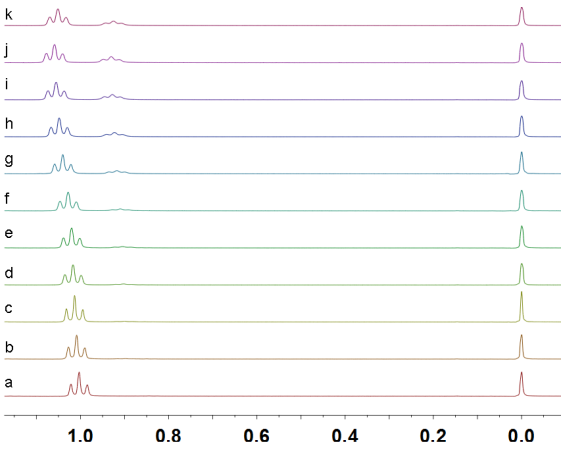

Fig. S18 Partial ^{1}H NMR spectra (400 MHz, $CDCl_3$, 22 °C) of **DPP5** at a constant concentration of 2.00 mM upon addition of **G** (**2g**, 15 mM): (a) 0.00 μL, (b) 10.0 μL to a, (c) 10.0 μL to b, (d) 10.0 μL to c, (e) 10.0 μL to d, (f) 25.0 μL to e, (g) 25.0 μL to f, (h) 25.0 μL to g, (i) 50.0 μL to h, (j) 50.0 μL to i, (k) 200 μL to j.

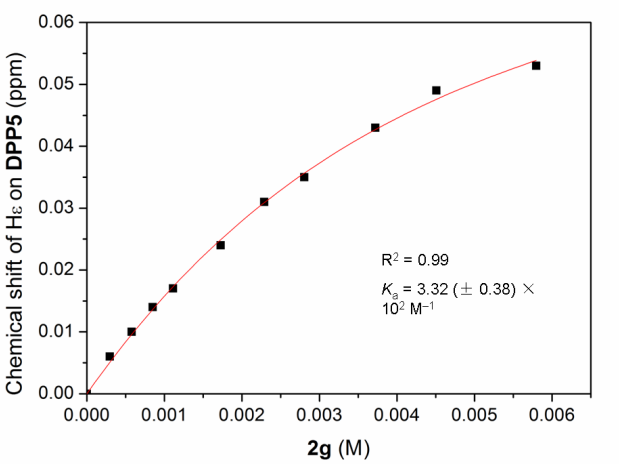

Fig. S19 The chemical shift changes of H_ε on **DPP5** upon addition of **2g**.

5. Mass spectrum of host–guest complexes

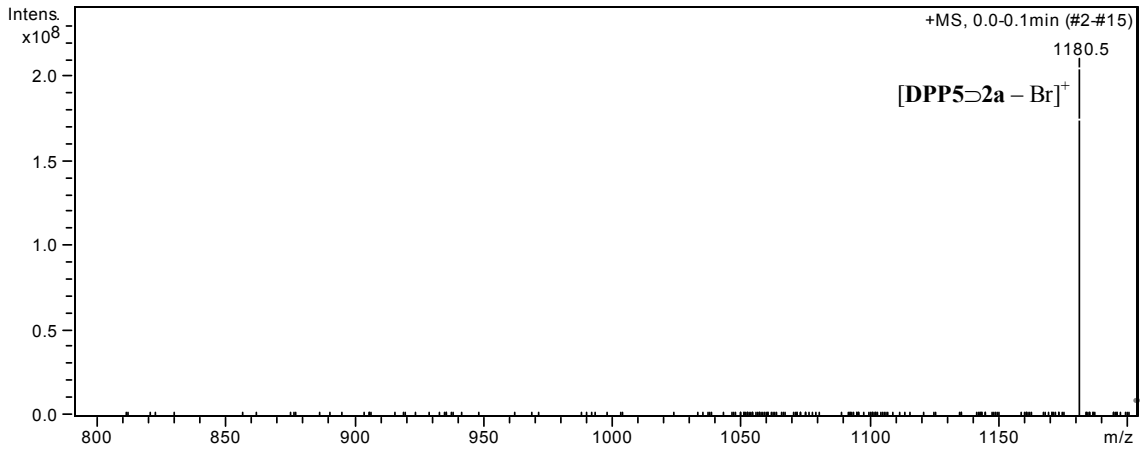

Fig. S20 Mass spectrum of the host–guest complex prepared from **DPP5** and **2a**.

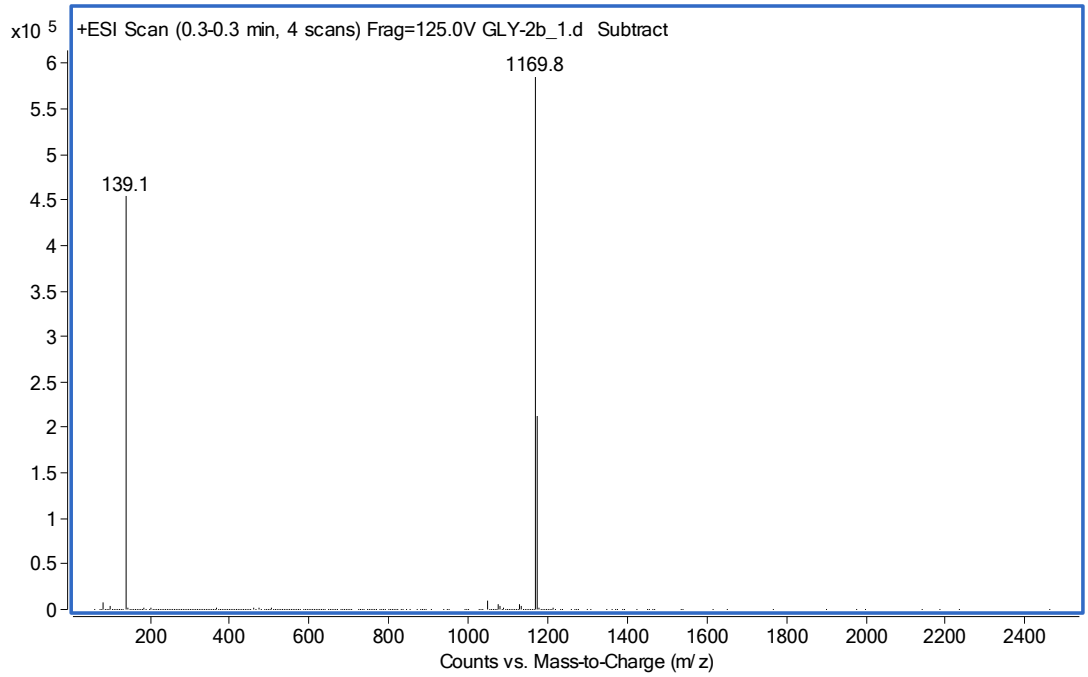

Fig. S21 Mass spectrum of the host–guest complex prepared from **DPP5** and **2b**.

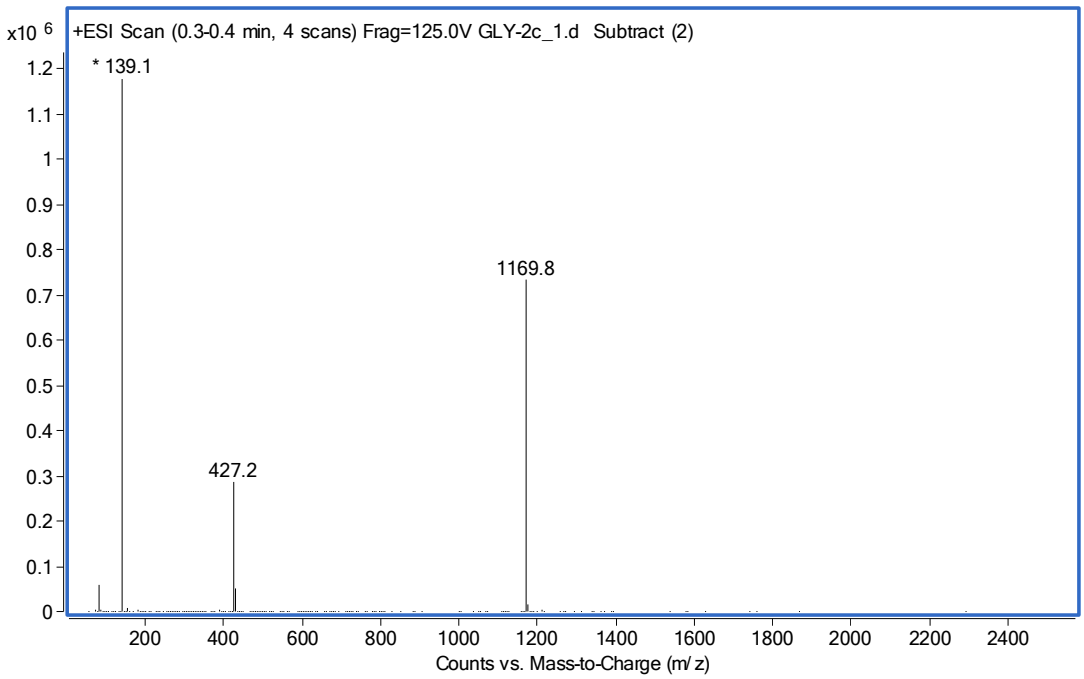

Fig. S22 Mass spectrum of the host–guest complex prepared from **DPP5** and **2c**.

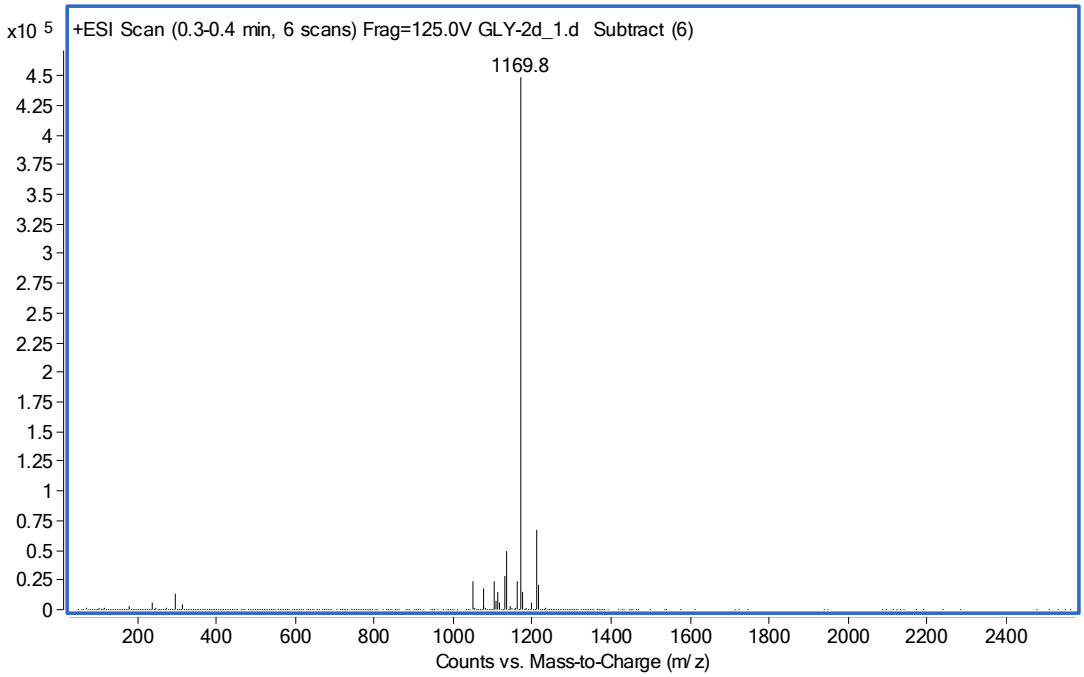

Fig. S23 Mass spectrum of the host–guest complex prepared from **DPP5** and **2d**.

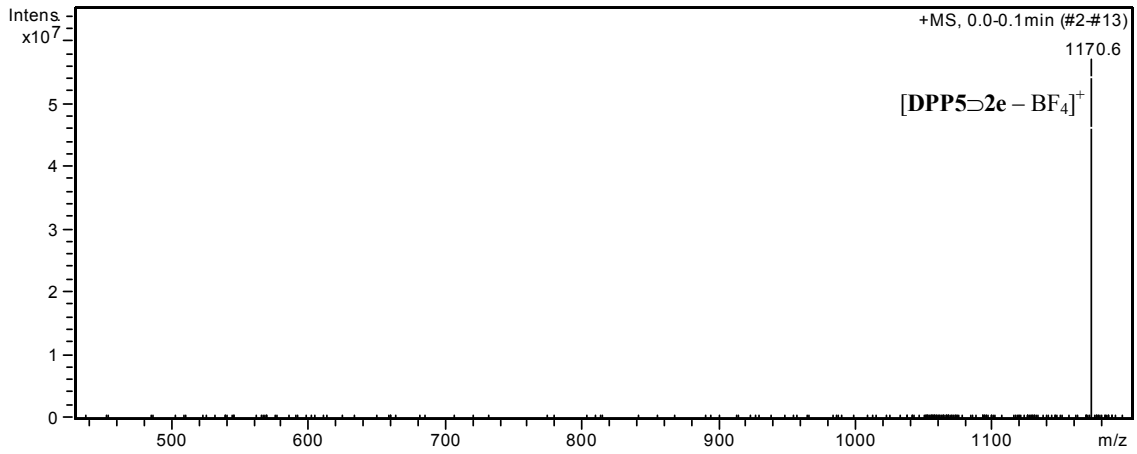

Fig. S24 Mass spectrum of the host–guest complex prepared from **DPP5** and **2e**.

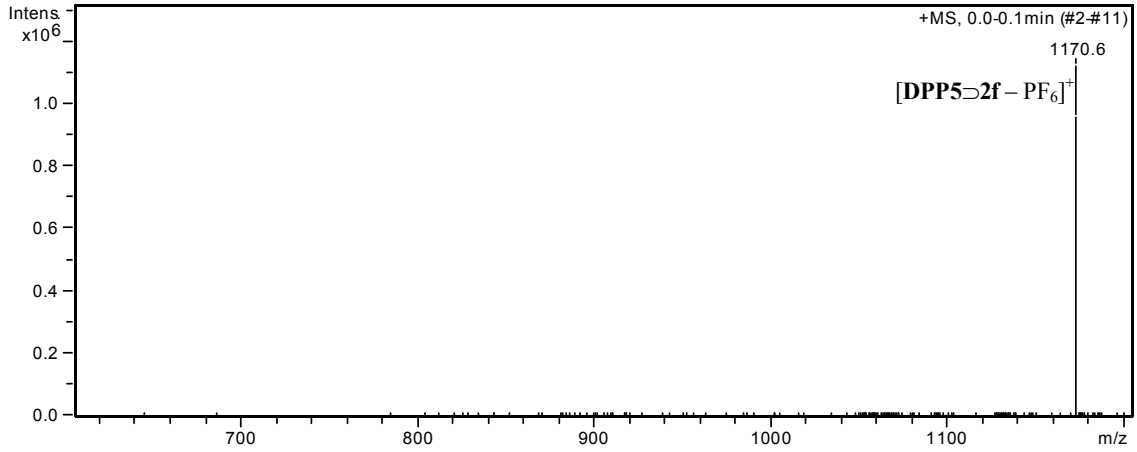

Fig. S25 Mass spectrum of the host–guest complex prepared from **DPP5** and **2f**.

*6. X-ray crystal data of **3***

Crystal data of ***3***: colorless, $C_{63}H_{80}F_{12}N_4O_{10}P_2$, *FW* 1342.25, Triclinic, space group P -1, a = 12.7806(6), b = 14.6895(6), c = 20.5104(10) Å, α = 110.228(4)°, β = 102.002(4)°, γ = 97.058(4)°, V = 3453.7(3) Å^3, Z = 2, D_c = 1.292 g cm^{-3}, T = 120(2) K, μ = 1.343 mm^{-1}, 21537 measured reflections, 12021 independent reflections, 831 parameters, 0 restraints, $F(000)$ = 1408, R_1 = 0.1166, wR_2 = 0.3021 (all data), R_1 = 0.0938, wR_2 = 0.2742 [$I > 2\sigma(I)$], max. residual density 0.932 e•Å^{-3}, and goodness-of-fit (F^2) = 1.130. CCDC-914822.

References:

S1. (*a*) R. Castro, K. R. Nixon, J. D. Evanseck and A. E. Kaifer, *J. Org. Chem.*, 1996, **61**, 7298–7303; (b) G. Yu, C. You, Z Zhang, J. Chen, X. Yan, B. Zheng, S. Liu and F. Huang, *J. Am. Chem. Soc.*, 2012, **134**, 8711–8717; (c) Y. Yao, M. Xue, X. Chi, Y. Ma, J. He, Z. Abliz and F. Huang, *Chem. Commun.*, 2012, **48**, 6505–6507.

S2. K. A. Connors, *Binding Constants*; Wiley: New York, 1987; P. S. Corbin, Ph.D. Dissertation, University of Illinois at Urbana-Champaign, Urbana, IL, 1999; P. R. Ashton, R. Ballardini, V. Balzani, M. Belohradsky, M. T. Gandolfi, D. Philp, L. Prodi, F. M. Raymo, M. V. Reddington, N. Spencer, J. F. Stoddart, M. Venturi and D. J. Williams, *J. Am. Chem. Soc.*, 1996, **118**, 4931–4951.